Multiple functions of liquid ferrate in the pretreatment of flue-gas desulfurization wastewater

Ruiyuan Zhang[a],*, Yunpeng Li[b], Qiujing Wang[a], Yu Song[a], Xuhui Sun[a], Mingyue Chen[b]

[a]*School of Chemistry Engineering, Northeast Electric Power University, Jilin 132012, Jilin, China,*
email: zhangry2780@163.com (R. Zhang)
[b]*Datang Changchun Third Thermal Power, Changchun 130000, Jilin, China*

ABSTRACT

The pretreatment of flue-gas desulfurization (FGD) wastewater directly affects the subsequent treatment effect of water. Liquid ferrate(VI) was used for the first time in the pretreatment of FGD wastewater. Influential factors including ferrate(VI) dosage and dosing method were investigated by batch tests. The results show that when the dosage of Na_2FeO_4 is 1.0 g/L, the removal rate of Mg^{2+}, Ca^{2+}, SO_4^{2-}, NH_4^+ and chemical oxygen demand were 99.80%, 83.09%, 7.24%, 28.72% and 26.46%, respectively. The strong oxidizing property of the liquid ferrate, the alkali therein, and the co-precipitation of the product promote the removal of these substances. Morphologic and element analysis confirmed that the composition of precipitates were $Fe_{16}O_{16}(SO_4)_2(OH)_{12} \cdot nH_2O$, FeO(OH), $CaSO_4$ and $Mg(OH)_2$. This paper provides a demonstration and theoretical guidance for the application of ferrate(VI) in FGD wastewater pretreatment.

Keywords: Flue-gas desulfurization wastewater; Ferrate(VI); Metal removal; SO_4^{2-} removal; Chemical oxygen demand removal

1. Introduction

Limestone-gypsum wet flue-gas desulfurization (FGD) technology has been widely employed in coal-fired power plants (CFPPs) to control SO_2 emissions [1,2]. The flue gas produced by burning coal mainly contains SO_x, NO_x, HCl, HF, and a small amount of heavy metals. After the flue gas is absorbed by the limestone aqueous solution in the desulfurization tower, desulfurization wastewater is formed, which mainly contains suspended solids, SO_3^{2-}, SO_4^{2-}, $S_2O_6^{2-}$, S^{2-}, F^-, Cl^-, NO_3^-, NO_2^-, and NH_4^+ remaining from the denitrification process [3]. The main component of limestone is $CaCO_3$, and it also contains various impurities such as MgO, Fe_2O_3, Al_2O_3, SiO_2, and a small amount of Hg, Cd, Cr, Pb, Ni, Zn, Cu, Mn, etc. The pH value of FGD wastewater is about 4–6, which is highly corrosive and highly toxic [4,5]. Due to the different origins of coal and limestone in each power plant, the composition of flue gas and wastewater produced varies greatly.

FGD wastewater is discharged periodically when the chloride concentration is higher than 20,000 mg/L to maintain desulfurization rate and prevent equipment corrosion [6,7]. Due to severe global water scarcity and aquatic environment pollution, zero-liquid discharge (ZLD) technology has received increasing attention since Chinese Government promulgated The Action Plan for Prevention and Treatment of Water Pollution in 2015 [8]. ZLD technology is a wastewater management strategy that eliminate liquid waste and promote water usage efficiency. Recently, mature FGD wastewater ZLD technologies mainly include thermal treatment (multi-effect distillation, mechanical vapor recompression, evaporative crystallization, bypass evaporation tower

* Corresponding author.

and flue evaporation) and membrane treatment (reverse osmosis, electrodialysis and membrane distillation) [9–13]. These ZLD technologies could recover most of water and solid products. However, large-scale applications of these technologies in CFPPs are limited by equipment clogging or corrosion caused by high-level impurities including large amounts of suspended solids, heavy metal ions, (Ca^{2+}, Mg^{2+}), Cl^- and SO_4^{2-} in FGD wastewater [14–17]. Therefore, FGD wastewater pretreatment is a necessary process for ZLD technologies.

The pretreatment goal of FGD wastewater is to reduce chemical oxygen demand (COD) and reduce the content of various metal ions and non-metal ions. The traditional pretreatment method is mainly a three-step process, namely: neutralization, flocculation or precipitation reaction, and sedimentation [6]. Neutralization and precipitation process are completed by adding alkali (NaOH, $Ca(OH)_2$ and other alkaline substances) and organic sulfur reagent (S^{2-} and TMT-15). The former substances could improve pH and remove Fe^{3+}, Cu^{2+}, Mg^{2+} and other metal ions, and the latter substances could react with Hg^{2+} and Pb^{2+} to form metal chelate precipitation [18]. Flocculation process aims to remove small particles and colloids through adding flocculants such as polyacrylamide and $FeCl_3$ [19,20].

These processes still have some drawbacks, such as high residual Cl^- and SO_4^{2-} concentrations, low removal rate of NH_4^+ and COD. To address these issues, many processing techniques have been developed. Struvite, ettringite and Friedel's salt were formed during the removal of NH_4^+, SO_4^{2-} and Cl^- from FGD wastewater [21–26]. In order to remove COD, oxidants such as sodium hypochlorite are often added. From the composition of FGD wastewater, pretreatment of FGD wastewater requires alkaline conditions and precipitants to remove metal ions, and an oxidant to remove COD. Liquid ferrate is exactly this kind of multifunctional water treatment agent. Ferrate(VI) is a recognized green oxidant with a redox potential ranging from 0.72–2.20 V under alkaline to acidic conditions [27,28]. Numerous studies have shown that ferrate can degrade organic pollutants [29–31] and kill viruses and bacteria [32,33]. The decomposition product $Fe(OH)_3$ of ferrate(VI) has the functions of flocculation and co-precipitation. Therefore, ferrate can also remove metal ions in water [34,35]. Liquid ferrate(VI) was self-made by electrolysis [36–38]. This product mainly contains high concentration of sodium hydroxide and ferrate(VI), which is just the right substitute of alkali, oxidant and precipitant for FGD wastewater pretreatment.

In this paper, the first attempt was made to treat FGD wastewater with liquid ferrate. Influential factors including ferrate(VI) dosage and dosing method were investigated by batch tests. Surface morphology of products were detected by scanning electron microscopy (SEM) and X-ray diffraction (XRD) coupled with VMinteq software which was used to calculate the precipitates at various pH values. The main objective of this study is to provide a demonstration and theoretical guidance for the application of ferrate(VI) in FGD wastewater pretreatment.

2. Materials and methods

2.1. Materials

FGD wastewater was collected from the third thermal power located in Changchun City, Jilin Province, P.R. China. The characteristics of the raw FGD wastewater are listed in Table 1. Liquid ferrate is a self-made product with a concentration between 0.08–0.16 mol/L. The liquid ferrate was prepared by electrolysis. The electrode used was sponge iron and electrolyte was sodium hydroxide. The cathode chamber and the anode chamber are separated by a diaphragm [28]. Different concentrations of liquid ferrate products were obtained with different duration of electrolysis. All the reagents used were analytical grade and provided by Sinopharm Chemical Reagent Co., Ltd., China.

2.2. Batch tests

Batch tests of FGD wastewater treatment were conducted employing a six-league electric blender (JBY 2, China) at room temperature 20°C~25°C. Ferrate(VI) was added into 500 mL of this wastewater under continuous stirring at a fast speed of 800 rpm for 1 min to ensure intensive mixing and then at a slow speed of 100 rpm for 15 min. The mixed liquor was settled for 12 h, and the supernatant were sampled for chemical analysis [36].

2.2.1. Effects of ferrate(VI) dosage

Five dosages (0.4, 0.6, 0.8, 1.0 and 1.2 g/L) were chosen to investigate ferrate(VI) dosage effects on the removal of Mg^{2+}, Ca^{2+}, SO_4^{2-}, NH_4^+ and COD. Five NaOH dosages (4, 6, 8, 10 and 12 g/L) were chosen to investigate NaOH dosage effects on the removal of Mg^{2+}, Ca^{2+}, SO_4^{2-}, NH_4^+ and COD.

2.2.2. Combined effect of ferrate concentration and alkalinity

To study the combined effect of ferrate and sodium hydroxide, ferrates were prepared at concentrations of 0.08, 0.10, 0.12, 0.14 and 0.16 mol/L, which contained varying

Table 1
Characteristics of flue-gas desulfurization wastewater

Properties	Concentration	Properties	Concentration
Ca^{2+}	1,111.68 mg/L	Turbidity	7.06 NTU
Mg^{2+}	2,182.32 mg/L	pH	7.14
Hardness	100.32 mmol/L	Conductivity	33.5 mS/cm
NH_4^+	4,784.42 mg/L	Cl^-	7,148.24 mg/L
Chemical oxygen demand	784.32 mg/L	SO_4^{2-}	15,084.46 mg/L

concentrations of sodium hydroxide. Generally, the longer the production time, the higher the ferrate concentration and the lower the sodium hydroxide concentration left in it. The NaOH concentration therein was determined by acid–base titration [5]. Treatment agents containing the same dose of ferrate but different amounts of sodium hydroxide were formulated from the above ferrate products.

2.3. Analysis methods

The pH and conductivity were measured by a pH meter (FE20, Mettler Toledo, China) and conductivity meter (DDS-307A, Leici, China). The colorimetric method was adopted for monitoring the NH_4^+, SO_4^{2-}, Ca^{2+} and Mg^{2+} concentrations [14]. Morphology and elemental composition of precipitates were observed by SEM (Hitachi SU8010, Japan) coupled with energy-dispersion spectroscopy. Composition of precipitates was analyzed using X-ray diffractometer (XRD) (40 kV, 40 mA, step size 0.1°, Rigaku Ultima IV, Japan), and the diffractograms of XRD were evaluated by Jade 6.

3. Results and discussion

3.1. Thermodynamic analysis

Fig. 1 illustrates the species calculated through VMinteq software at simulated FGD wastewater. Fig. 1a shows the effects of pH on precipitation from Mg^{2+}-Ca^{2+}-SO_4^{2-}-H_2O system containing 0.1 mol/L Mg^{2+}, 0.03 mol/L Ca^{2+} and 0.15 mol/L SO_4^{2-} in various pH solutions. The mainly species were $MgSO_4$ (aq), $CaSO_4$ (aq), $Mg(OH)^+$, $Ca(OH)^+$, $Mg(OH)_2$ and $Ca(OH)_2$. The proportion of SO_4^{2-}, $MgSO_4$ (aq) and $CaSO_4$ (aq) in raw FGD wastewater were 41.52%, 31.70% and 10.66%, respectively. The concentration of Mg^{2+} and $MgSO_4$ (aq) reduced when the pH value was greater than 9.5 which corresponds to the formation of $Mg(OH)_2$. The concentration of $Mg(OH)^+$ and $Ca(OH)^+$ increased sharply when the pH value were higher than 8.5 and 10.5, respectively. Meanwhile, large amount of $Ca(OH)_2$ were formed at pH 13.0 resulting the

reduction of Ca^{2+} and $CaSO_4$ (aq). As shown in Fig. 1b, the effects of pH on precipitation at Mg^{2+}-Ca^{2+}-SO_4^{2-}-NH_4^+-H_2O system containing 0.18 mol/L NH_4^+. The proportion of NH_4^+ gradually decreased when pH value higher than 7.5. On the contrary, more and more NH_3 (aq) were formed from pH 5.0. In addition, the concentration of Ca^{2+} was seriously affected by NH_4^+, which formed $Ca(NH_3)_2^{2+}$ and $Ca(NH_3)^{2+}$.

3.2. Effects of ferrate(VI) dosage

Fig. 2 illustrates the effects of ferrate(VI) dosage on pH value and the removal rate of Ca^{2+} and Mg^{2+}. The pH value slowly increased when the dosage is lower than 0.8 g/L, then sharply increased to 13.1. The residual concentration of Ca^{2+} and Mg^{2+} decreased with the increase of pH value. The results of theoretical calculation deduced that $Mg(OH)_2$ precipitates were formed when the pH value is greater than 9.5. The largest negative zeta potential was attained at pH
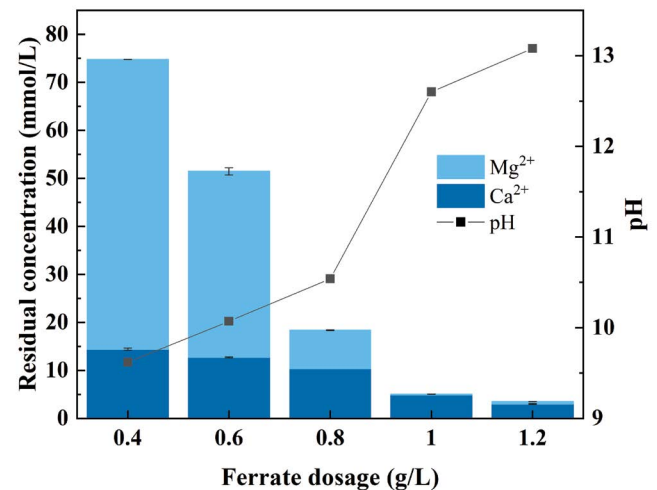

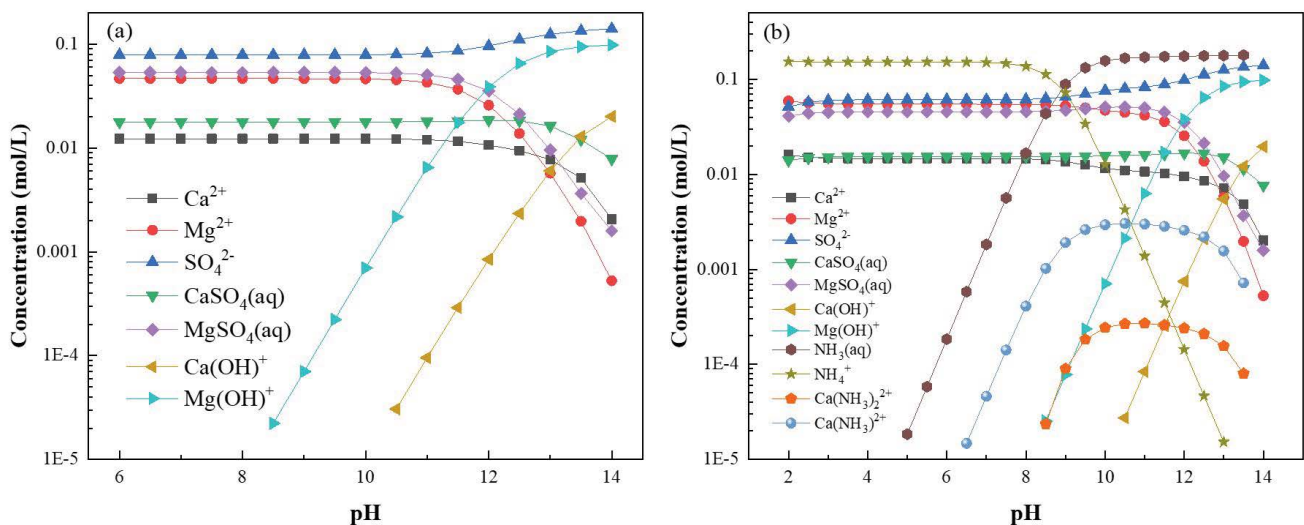Fig. 2. Influences of ferrate(VI) dosage on pH, Ca^{2+} and Mg^{2+}.

Fig. 1. Effects of pH on speciation in simulated flue-gas desulfurization wastewater. (a) Mg^{2+}-Ca^{2+}-SO_4^{2-}-H_2O system and (b) Mg^{2+}-Ca^{2+}-SO_4^{2-}-NH_4^+-H_2O system.

11.5 [39]. The removal rate of Ca^{2+} and Mg^{2+} were 89.11% and 99.35%, respectively. However, the concentration of Ca^{2+} remained basically at 3.02 mmol/L which indicated that the dominant phase of precipitate was $Mg(OH)_2$. When the dosage is larger than 1.0 g/L, the residual concentration of Mg^{2+} in the solution was almost zero and the residual OH^- was retained in the solution which greatly increased the pH value. This result indicated that a high removal rate of Ca^{2+} and Mg^{2+} was achieved when the ferrate dosage was 1.0 g/L and pH was 12.6.

Fig. 3 shows the removal rate of SO_4^{2-}, NH_4^+ and COD with ferrate(VI) dosage. The removal rate of SO_4^{2-} increased with the increasing dosage. When the dosage was 1.2 g/L, the removal rate of SO_4^{2-} was 8.26% and the corresponding decreased concentration of SO_4^{2-} was 1,245.58 mg/L which was due to the formation of schwertmannite ($Fe_{16}O_{16}(SO_4)_2(OH)_{12} \cdot nH_2O$) and calcium sulfate. As the dosage of ferrate(VI) increased from 0.4 to 1.2 g/L, the removal rate of NH_4^+ increased from 15.06% to 31.92%, and the removal rate of COD increased from 6.71% to 31.41%. The corresponding pH increased from 9.6 to 13.1, as shown in Fig. 2. NH_4^+ in FGD wastewater comes from the denitrification process in CFPPs. In order to improve the effect of nitrogen removal, excessive ammonia was added [21]. A large amount of NH_4^+ reacted with OH^- to form ammonia and then escaped from the solution. This is consistent with thermodynamic analysis. COD in the FGD wastewater could be removed by oxidation because of the composition of COD were thiosulfate, sulfite and rhodanate [20]. The more ferrate(VI) dosage added, the more reducing substances could be oxidized.

Alkali plays an important role in removing metal ions and ammonia, so the effect of NaOH concentration in the absence of ferrate was investigated. The amount of NaOH added is consistent with the amount of residual alkali in the ferrate(VI) treatment. Fig. 4 illustrates the variations of Mg^{2+}, Ca^{2+}, SO_4^{2-}, NH_4^+ and COD removal rate with different NaOH dosage. All curves show an increasing tendency with enhancing NaOH dosage. The removal rate of Mg^{2+} increased from 12.49% to 100% when the dosage gradually increased to 12 g/L. The removal rate of Mg^{2+} was similar

in ferrate treatment and alkali treatment. The Ca^{2+} removal rate of alkali treatment was 80.32% which was lower than ferrate treatment. However, the removal rates of SO_4^{2-} and COD did not change significantly with NaOH dosage in alkali treatment. The removal rates of SO_4^{2-} and COD were only 3.21% and 4.91% when the NaOH dosage was 12 g/L. The COD removal rate of ferrate treatment was 26.46% which was three times higher than that of alkali treatment. This is mainly because ferrate(VI) has high oxidation ability and can remove COD. The removal rate of NH_4^+ increased from 6.31% to 40.21%. It was shown that NaOH solution was more conducive to the formation of ammonia. In addition, ferrate(VI) has flocculation properties equivalent to the addition of coagulants, resulting in faster and denser precipitation.

3.3. Combined effect of ferrate concentration and alkalinity

It can be seen from the above experimental results that the concentration of ferrate(VI) and the concentration of NaOH are both important factors affecting the treatment effect. Therefore, it is necessary to investigate the effects of different amount of OH^- on the removal rates of Mg^{2+}, Ca^{2+} and SO_4^{2-} under the same ferrate dosage. Ferrates were prepared at concentrations of 0.08, 0.10, 0.12, 0.14 and 0.16 mol/L, which contained varying concentrations of sodium hydroxide. Generally, the longer the production time, the higher the ferrate concentration and the lower the sodium hydroxide concentration left in it.

As shown in Fig. 5, when the dosage of ferrate is 1.0 g/L, with the decrease of pH value, the removal rate of SO_4^{2-} gradually increases, while the removal rate of Ca^{2+} and Mg^{2+} gradually decreases. The formation of metal ion hydrolysis precipitates is closely related to the OH^- concentration, which is mainly reflected in the pH value of the solution. When the alkalinity of the solution decreases, the oxidizing ability of ferrate increases, so more sulfite is oxidized to sulfate. While sulfate is removed under neutral or weakly acidic conditions due to the easy formation of schwertmannite
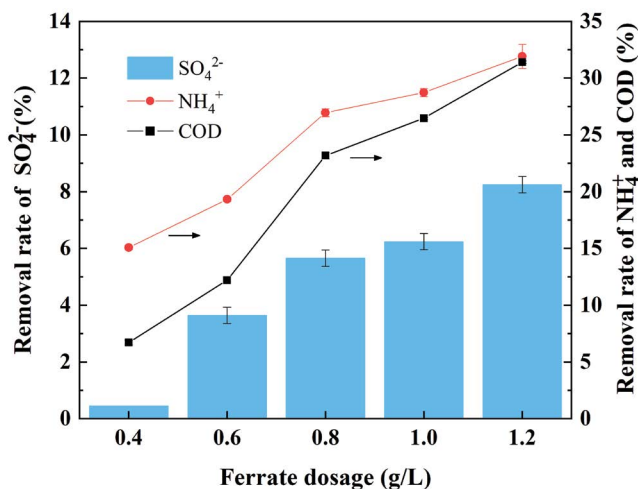

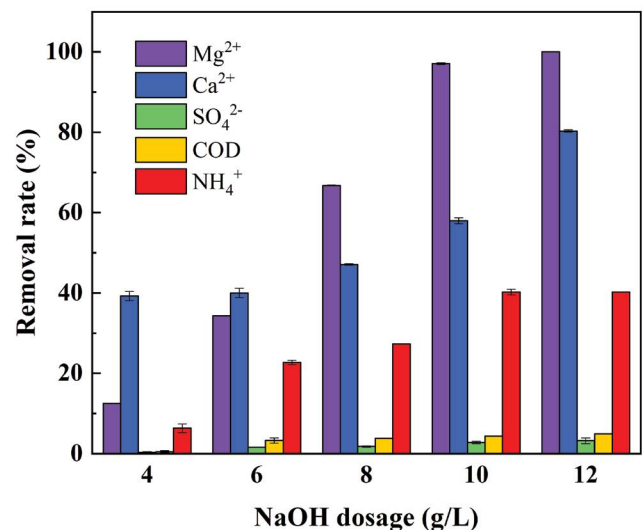Fig. 3. Influences of ferrate(VI) dosage on SO_4^{2-}, NH_4^+ and chemical oxygen demand.

Fig. 4. Influences of NaOH dosage on Mg^{2+}, Ca^{2+}, SO_4^{2-}, NH_4^+ and chemical oxygen demand.

precipitation. Therefore, the lower the alkalinity, the more favorable it is to remove sulfate.

Fig. 6 illustrates the effects of ferrate(VI) concentration on the removal rate of NH_4^+ and COD. As shown in Fig. 6a, under the condition of fixed ferrate(VI) concentration, the NH_4^+ removal rate increased gradually with the increase of pH value. These results were consistent with Cheng et al. [14], who reported that NH_4^+ removal rate was related to the solution pH value. The same dose of treatment agent prepared with high-concentration ferrate products contains a lower concentration of sodium hydroxide, so the removal rate of ammonia is also lower. The variation of COD removal rate is opposite to NH_4^+. The higher the acidity, the higher the redox potential of ferrate and the stronger the oxidizing ability. As shown in Fig. 6b, the same dose of treatment agent prepared from high-concentration ferrate products contains a lower concentration of sodium hydroxide, so the removal rate of COD is higher.
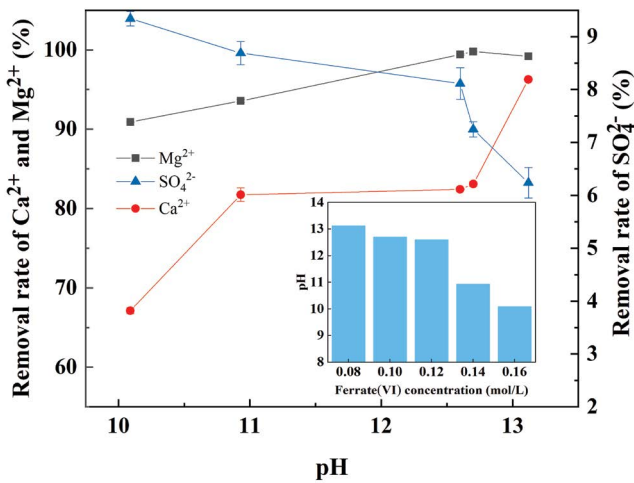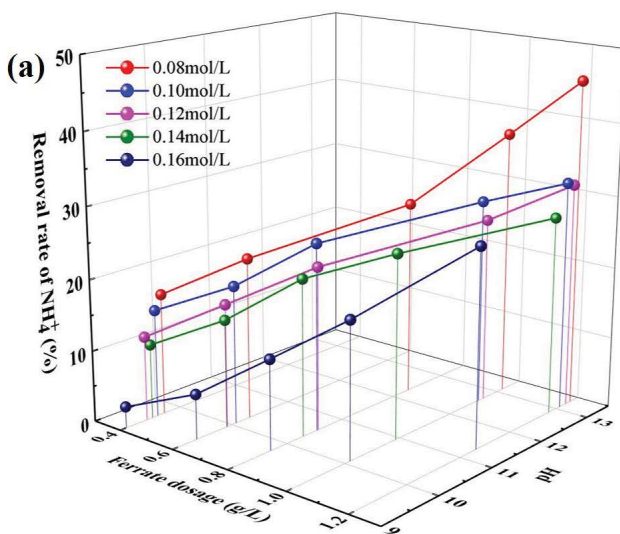

Fig. 5. Effects of different pH values on the removal rates of Mg^{2+}, Ca^{2+} and SO_4^{2-} under the same ferrate dosage.

3.4. Effects of dosing way

Since a large amount of precipitation was generated when ferrate(VI) was added, the effect of adding it in parts was examined. Models 1, 2 and 3 were performed by adding the same amount of ferrate(VI) to 1 L of FGD wastewater in ten, five and two times, respectively. After each addition of ferrate(VI), remove the precipitate and re-dosing. The concentration of raw material ferrate(VI) used is 0.1 mol/L. The results are shown in Fig. 7.

The higher pH value was achieved by Mode 1 which have more batch times of dosing process. However, the removal rate of hardness ions were different as shown in Fig. 7b. The removal rate of hardness ions was less than 46% when ferrate(VI) dosage was below 0.6 g/L and the corresponding pH value was only around 10. When the dosage was higher than 0.8 g/L, the removal rate of hardness ions sharply increased to 98%. Large amount of white precipitate was found indicating that $Mg(OH)_2$ precipitate was formed at this stage.

Fig. 7c illustrates the variation of SO_4^{2-} removal rate at different dosing ways. All three dosing modes proved that increasing ferrate(VI) dosage could increase the removal rate of SO_4^{2-}. Under the condition of ferrate concentration of 1.0 g/L, the SO_4^{2-} removal rate in Modes 1, 2 and 3 was 13.43%, 7.18% and 5.52%, respectively. This is because the amount of NaOH introduced each time is less when it is added in multiple times. Under the condition of low alkalinity, the ferrate(VI) has a stronger oxidation ability, and it is easier to form the precipitate of the schwertmannite containing sulfate. As shown in Fig. 7d, NH_4^+ removal rate of Mode 1 rapidly increased to 69.15% at ferrate(VI) dosage 1.0 g/L which was higher than that in Sections 3.2 – Effects of ferrate(VI) dosage and 3.3 – Combined effect of ferrate concentration and alkalinity. It was because Mode 1 could make more efficient utilization of residual alkali in ferrate(VI) solution. In addition, filtration was employed to separate the precipitate and solution during the test, which makes more contact with air and more volatile. This method could improve removal rate of NH_4^+ [14].
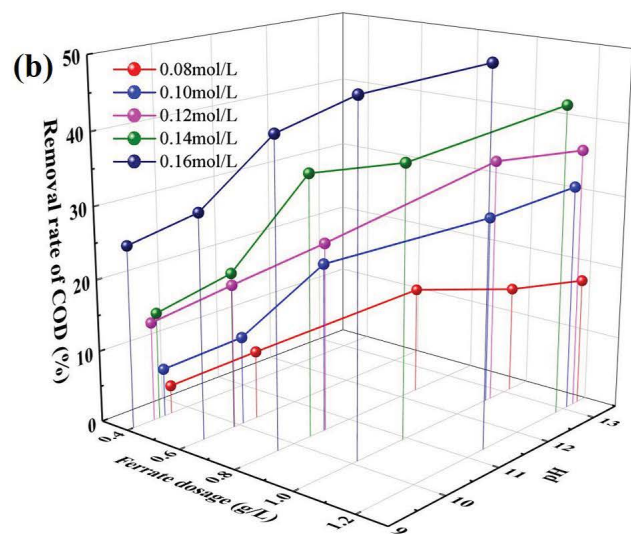

Fig. 6. Influences of ferrate(VI) concentration on the removal rate of NH_4^+ (a) and chemical oxygen demand (b).
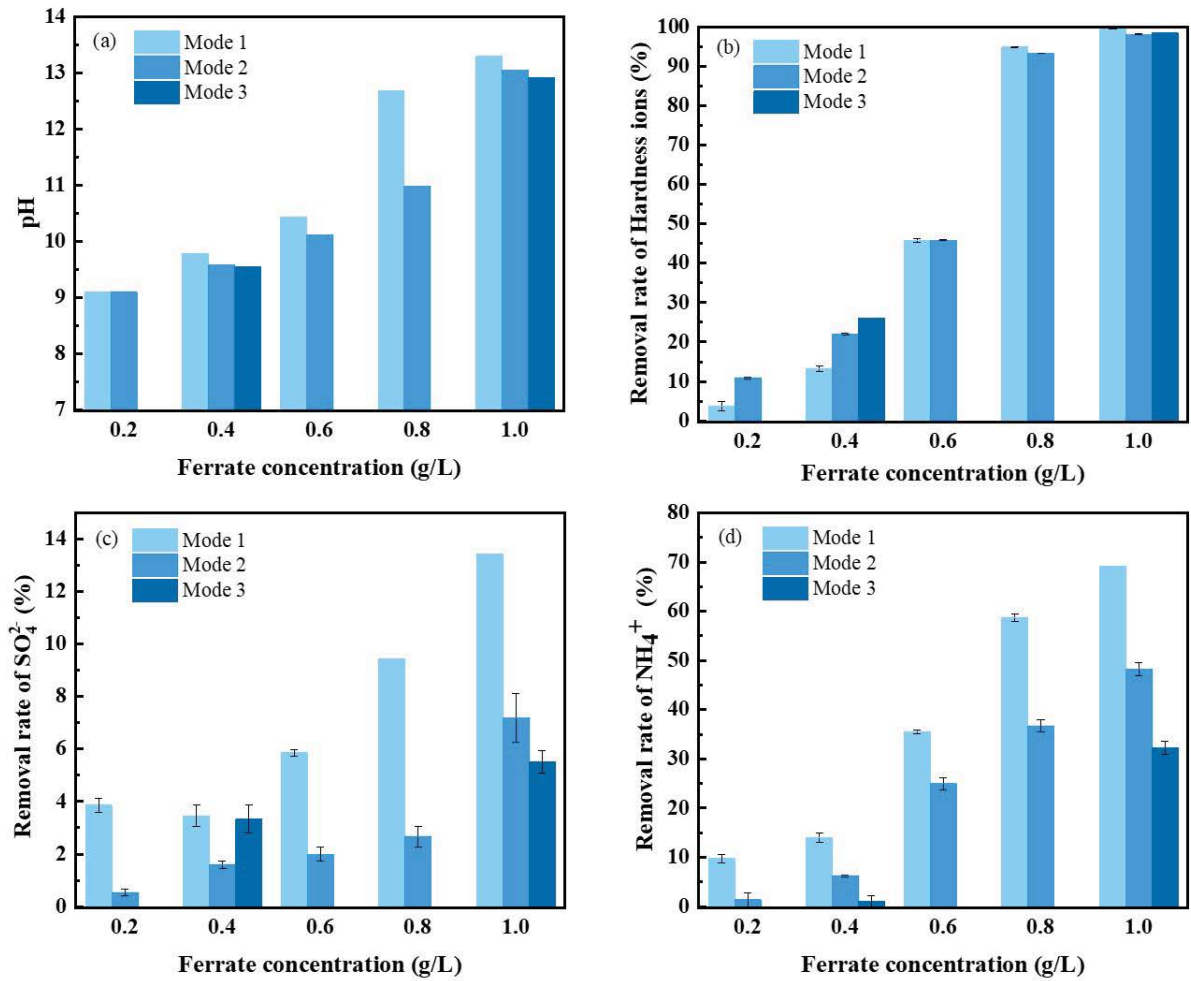
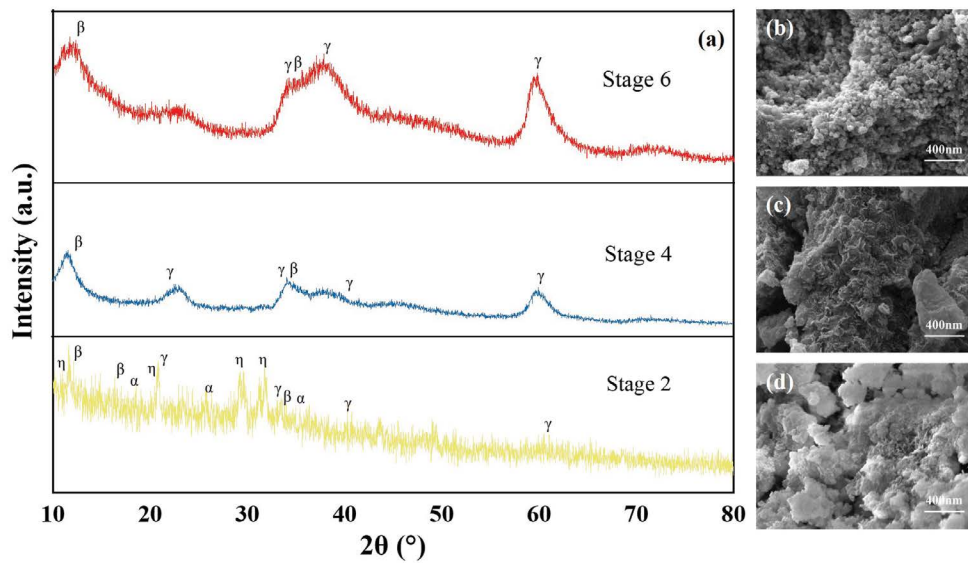Fig. 7. Influences of dosing ways on pH and removal rate of hardness ions, SO_4^{2-} and NH_4^+.

Fig. 8. X-ray diffraction patterns and scanning electron microscopy images of precipitates obtained from Mode 1. (a) X-ray diffraction patterns (α-$Fe_{16}O_{16}(SO_4)_2(OH)_{12}\cdot nH_2O$, β-FeO(OH), γ-$Mg(OH)_2$, η-$CaSO_4$), scanning electron microscopy image of (b) stage 2, (c) stage 4, and (d) stage 6.

Table 2
Chemical composition of precipitates in Mode 1 obtained by energy-dispersive X-ray spectroscopy (wt.%)

Element	O	Mg	S	Ca	Fe
Stage 2	17.98	28.37	5.70	28.19	19.74
Stage 4	17.79	62.58	6.31	5.26	8.03
Stage 6	14.43	68.02	7.55	2.41	7.58

3.5. Morphology and element analysis of precipitates

XRD, SEM and energy-dispersive X-ray spectroscopy (EDS) analyses were conducted to analyze the composition of precipitates obtained from Mode 1. As shown in Fig. 8a, XRD pattern of precipitates reveals the main peaks at d = 4.86, 3.39 and 2.55 Å of schwertmannite, at d = 7.41, 5.24 and 2.54 Å of FeO(OH), at d = 7.63, 4.28, 3.06 and 2.87 Å of $CaSO_4$ and at d = 4.35, 2.63, 2.25 and 1.52 Å of $Mg(OH)_2$ in stage 2 [23]. XRD results illustrated that peak intensities of $Mg(OH)_2$ increased with adding more ferrate(VI), which led to the increase of pH value in the solution and enhanced the proportion of $Mg(OH)_2$ in the precipitate. SEM image in Fig. 8b showed that the crystal morphology of precipitate from stage 2 was spherical shape, which was consistent with the morphological characteristics of schwertmannite [40]. Fig. 8a and Table 2 show that iron and magnesium were observed with increasing ferrate(VI) dosage, indicating FeO(OH) and $Mg(OH)_2$ were formed in stage 4.

XRD pattern of precipitates from stage 6 reveals the three main peaks of $Mg(OH)_2$ located at d = 2.63, 2.37 and 1.52 Å. This proved that Mg^{2+} was removed as lamella-like $Mg(OH)_2$ precipitates (Fig. 8d) in stage 6. The EDS analysis (Table 2) provided further proof that large amount of magnesium was detected in the precipitates.

4. Conclusions

Batch results showed that Ca^{2+}, Mg^{2+}, SO_4^{2-}, NH_4^+ and COD were efficiently removed from FGD wastewater by adding ferrate(VI). The COD removal rate could be increased by enhancing ferrate(VI) concentration, while the other pollutants would be reduced. The removal rate of Mg^{2+}, Ca^{2+}, SO_4^{2-}, NH_4^+ and COD were 99.80%, 83.09%, 7.24%, 28.72% and 26.46% at optimized ferrate(VI) dosage 1.0 g/L. The batch dosing could improve the utilization of ferrate(VI) effectively. Morphologic and element analysis confirmed that the composition of precipitates were schwertmannite, FeO(OH), $CaSO_4$ and $Mg(OH)_2$. Ferrate(VI) treatment was a technically and economically feasible way for FGD wastewater pretreatment in CFPPs.

Author contributions

Writing—original draft, Y.L.; Methodology, Writing–X.S.; Writing—review & editing, Q.W., Y.S. and M.C.; Conceptualization, and writing—review & editing, R.Z.

Funding

References

[1] P. Córdoba, Status of flue gas desulphurisation (FGD) systems from coal-fired power plants: overview of the physic-chemical control processes of wet limestone FGDs, Fuel, 144 (2015) 274–286.
[2] X. Liu, B. Lin, Y. Zhang, Sulfur dioxide emission reduction of power plants in China: current policies and implications, J. Cleaner Prod., 113 (2016) 133–143.
[3] X. Liu, H. Zhang, X. Zhang, Y. Yang, C. Yang, P. Zhao, Y. Dong, Chloride removal from flue-gas desulfurization wastewater through Friedel's salt precipitation method: a review, Sci. Total Environ., 862 (2023) 160906, doi: 10.1016/j.scitotenv.2022.160906.
[4] Z. Zhou, Q. Zhu, Z. Lan, Y. Yang, L. Zeng, C. Liu, J. Guo, X. Zhao, Insights into chloride sorption and phase transformation of the synthesized Ca-Al bimetallic oxides in flue-gas desulfurization wastewater, Chem. Eng. J., 475 (2023) 146214, doi: 10.1016/J.CEJ.2023.146214.
[5] R. Zhang, Y. Song, Y. Li, Y. Yang, X. Sun, Y. Li, Treatment of flue-gas desulfurization wastewater by bipolar membrane electrodialysis and its optimization by response surface methodology, Desal. Water Treat., 270 (2022) 25–34.
[6] S. Ma, J. Chai, K. Wu, Y. Xiang, S. Jia, Q. Li, Experimental research on bypass evaporation tower technology for zero liquid discharge of desulfurization wastewater, Environ. Technol., 40 (2019) 2715–2725.
[7] S. Ma, J. Chai, G. Chen, W. Yu, S. Zhu, Research on desulfurization wastewater evaporation: Present and future perspectives, Renewable Sustainable Energy Rev., 58 (2016) 1143–1151.
[8] S. Ma, J. Chai, G. Chen, K. Wu, Y. Xiang, Z. Wan, H. Zhu, Partitioning characteristic of chlorine ion in gas and solid phases in process of desulfurization wastewater evaporation: model development and calculation, Environ. Sci. Pollut. Res., 26 (2019) 8257–8265.
[9] H. Zheng, C. Zheng, X. Li, S. Xu, S. Liu, Y. Zhang, W. Weng, X. Gao, Evaporation and concentration of desulfurization wastewater with waste heat from coal-fired power plants, Environ. Sci. Pollut. Res., 26 (2019) 27494–27504.
[10] S. Lee, Y. Kim, S. Hong, Treatment of industrial wastewater produced by desulfurization process in a coal-fired power plant via FO-MD hybrid process, Chemosphere, 210 (2018) 44–51.
[11] D.B. Gingerich, E. Grol, M.S. Mauter, Fundamental challenges and engineering opportunities in flue-gas desulfurization wastewater treatment at coal fired power plants, Environ. Sci. Water Res. Technol., 4 (2018) 909–925.
[12] Y. Muhammad, W. Lee, Zero-liquid discharge (ZLD) technology for resource recovery from wastewater: a review, Sci. Total Environ., 681 (2019) 551–563.
[13] T. Tong, M. Elimelech, The global rise of zero liquid discharge for wastewater management: drivers, technologies, and future directions, Environ. Sci. Technol., 50 (2016) 6846–6855.
[14] Q. Cheng, Y. Wu, Y. Huang, F. Li, Z. Liu, L. Nengzi, L. Bao, An integrated process of calcium hydroxide precipitation and air stripping for pretreatment of flue-gas desulfurization wastewater towards zero liquid discharge, J. Cleaner Prod., 314 (2021) 128077, doi: 10.1016/j.jclepro.2021.128077.
[15] C. Zheng, H. Zheng, Z. Yang, S. Liu, X. Li, Y. Zhang, W. Weng, X. Gao, Experimental study on the evaporation and chlorine migration of desulfurization wastewater in flue gas, Environ. Sci. Pollut. Res., 26 (2019) 4791–4800.
[16] Z. Liang, Y. Yan, J. Yan, T. Lee, Z. Yang, L. Zhang, C. Lee, The study of evaporation characteristics of the desulfurization wastewater (electrolyte solution) droplet, Appl. Therm. Eng., 161 (2019) 114119, doi: 10.1016/j.applthermaleng.2019.114119.
[17] Z. Sun, L. Yang, S. Chen, L. Bai, X. Wu, Promoting the removal of fine particles and zero discharge of desulfurization wastewater by spray-turbulent agglomeration, Fuel, 270 (2020) 117461, doi: 10.1016/j.fuel.2020.117461.

[18] X. Han, D. Zhang, J. Yan, S. Zhao, J. Liu, Process development of flue gas desulphurization wastewater treatment in coal-fired power plants towards zero liquid discharge: energetic, economic and environmental analyses, J. Cleaner Prod., 261 (2020) 121144, doi: 10.1016/j.jclepro.2020.121144.

[19] M. Xia, C. Ye, K. Pi, D. Liu, A. Gerson, Ca removal and Mg recovery from flue-gas desulfurization (FGD) wastewater by selective precipitation, Water Sci. Technol. ,76 (2017) 2842–2850.

[20] W. Dou, Z. Zhou, J. Ye, R. Huang, L. Jiang, G. Chen, X. Fei, Reusing effluent of flue-gas desulfurization wastewater treatment process as an economical calcium source for phosphorus removal, Water Sci. Technol., 76 (2017) 1429–1435.

[21] X. Zhao, C. Tu, Z. Zhou, W. Zhang, X. Ma, J. Yang, Recovery of ammonia nitrogen and magnesium as struvite from wastewaters in coal-fired power plant, Asia-Pac. J. Chem. Eng., 14 (2019), doi: 10.1002/apj.2355.

[22] J. Yu, J. Lu, Y. Kang. Removal of sulfate from wet FGD wastewater by co-precipitation with calcium hydroxide and sodium aluminate, Water Sci. Technol., 77 (2018) 1336–1345.

[23] J. Guo, Z. Zhou, Q. Ming, D. Sun, F. Li, J. Xi, Q. Wu, J. Yang, Q. Xia, X. Zhao, Recovering chemical sludge from the zero liquid discharge system of flue gas desulfurization wastewater as flame retardants by a stepwise precipitation process, J. Hazard. Mater., 417 (2021) 126054, doi: 10.1016/j.jhazmat.2021.126054.

[24] X. Tian, Z. Zhou, Y. Xin, L. Jiang, X. Zhao, Y. An, A novel sulfate removal process by ettringite precipitation with aluminum recovery: kinetics and a pilot-scale study, J. Hazard. Mater., 365 (2019) 572–580.

[25] Y. Xin, Z. Zhou, Q. Ming, D. Sun, J. Han, X. Ye, S. Dai, L. Jiang, X. Zhao, L. An, A two-stage desalination process for zero liquid discharge of flue-gas desulfurization wastewater by chloride precipitation, J. Hazard. Mater., 397 (2020) 122744, doi: 10.1016/j.jhazmat.2020.122744.

[26] X. Ye, X. Zhao, Q. Ming, J. Zhu, J. Guo, D. Sun, S. Zhang, J. Xu, Z. Zhou, Process optimization to enhance utilization efficiency of precipitants for chloride removal from flue-gas desulfurization wastewater via Friedel's salt precipitation, J. Environ. Manage., 299 (2021) 113682, doi: 10.1016/j.jenvman.2021.113682.

[27] V.K. Sharma, R. Zboril, R.S. Varma, Ferrates: greener oxidants with multimodal action in water treatment technologies, Acc. Chem. Res., 48 (2015) 182–191.

[28] X. Sun, Q. Zhang, H. Liang, Y. Li, X. Meng, V.K. Sharma, Ferrate(VI) as a greener oxidant: electrochemical generation and treatment of phenol, J. Hazard. Mater., 319 (2016) 130–136.

[29] P. Kovalakova, L. Cizmas, M. Feng, T.J. McDonald, B. Marsalek, V.K. Sharma, Oxidation of antibiotics by ferrate(VI) in water: evaluation of their removal efficiency and toxicity changes, Chemosphere, 277 (2021) 130365, doi: 10.1016/j.chemosphere.2021.130365.

[30] X. Sun, M. Feng, S. Dong, Y. Qi, L. Sun, N. Nasri, V.K. Sharma, Removal of sulfachloropyridazine by ferrate(VI): kinetics, reaction pathways, biodegradation, and toxicity evaluation, Chem. Eng. J., 372 (2019) 742–751.

[31] J. Chen, X. Xu, X. Zeng, M. Feng, R. Qu, Z. Wang, N. Nesnas, V.K. Sharma, Ferrate(VI) oxidation of polychlorinated diphenyl sulfides: kinetics, degradation, and oxidized products, Water Res., 143 (2018) 1–9.

[32] L. Zheng, J. Cui, Y. Deng. Emergency water treatment with combined ferrate(VI) and ferric salts for disasters and disease outbreaks, Environ. Sci. Water Res. Technol., 6 (2020) 2816–2831.

[33] K. Manoli, R. Maffettone, V.K. Sharma, D. Santoro, A.K. Ray, K.D. Passalacqua, K.E. Carnahan, C.E. Wobus, S. Saeathy, Inactivation of murine norovirus and fecal coliforms by ferrate(VI) in secondary effluent wastewater, Environ. Sci. Technol., 54 (2020) 1878–1888.

[34] J. Kolarík, R. Prucek, J. Tucek, J. Filip, K.V. Sharma, R. Zbořil, Impact of inorganic ions and natural organic matter on arsenates removal by ferrate(VI): understanding a complex effect of phosphates ions, Water Res., 141 (2018) 357–365.

[35] J.E. Goodwill, J. LaBar, D. Slovikosky, H.J.W. Strosnider, Preliminary assessment of ferrate treatment of metals in acid mine drainage, J. Environ. Qual., 48 (2019) 1549–1556.

[36] X. Sun, K. Zu, H. Liang, L. Sun, L. Zhang, C. Wang, V.K. Sharma, Electrochemical synthesis of ferrate(VI) using sponge iron anode and oxidative transformations of antibiotic and pesticide, J. Hazard. Mater., 344 (2018) 1155–1164.

[37] R. Pi, H. Liu, X. Sun, R. Zhang, J. Zhang, V.K. Sharma, Strategy of periodic reverse current electrolysis to synthesize ferrate(VI): enhanced yield and removal of sulfachloropyridazine, Sep. Purif. Technol., 263 (2021) 118420, doi: 10.1016/j.seppur.2021.118420.

[38] R. Tong, P. Zhang, Y. Yang, R. Zhang, X. Sun, X. Ma, V.K. Sharma, Online continuous chemical synthesis of ferrate(VI): enhanced yield and removal of pollutants, J. Environ. Chem. Eng., 9 (2021) 106512, doi: 10.1016/j.jece.2021.106512.

[39] H. Schott, Electrokinetic studies of magnesium hydroxide, J. Pharm. Sci., 70 (1981) 486–489.

[40] X. Su, X. Li, L. Ma, J. Fan, Formation and transformation of schwertmannite in the classic Fenton process, J. Environ. Sci., 82 (2019) 145–154.